Authors' Accepted Manuscript (*J. Comput. Civ. Eng.*, 2020, 34(3): 04020003)

Feasible Prestress Modes for Cable-Strut Structures with Multiple Self-Stress States Using Particle Swarm Optimization

Yao Chen, M. ASCE, Ph. D.[1]; Jiayi Yan[2]; Pooya Sareh, Ph. D.[3]; Jian Feng, Ph. D.[4]

Abstract

A prestressed cable-strut structure is usually regarded as a mechanism before being prestressed. Under the action of initial prestresses, the internal infinitesimal mechanisms can be rigidified, resulting in achieving the desired structural stiffness. Therefore, feasible prestress design is a key to develop and analyze novel prestressed cable-strut structures. In this study, an effective optimization method is presented to determine the optimal feasible prestress modes of a cable-strut structure with predefined geometry and multiple self-stress states. Two optimization models based on the self-stress states and the integral self-stress states are presented to compute the optimal feasible prestress modes. Thereafter, the multi-objective optimization problem is converted into a single objective optimization problem by the weight coefficient method, and the particle swarm optimization algorithm is applied to find feasible solutions. Illustrative examples verify the feasibility of the presented optimization algorithms to calculate feasible prestress modes. In comparison with the conventional optimization methods, the proposed method shows satisfactory accuracy and efficiency.

Keywords: Cable-strut structure; Force-finding; Feasible prestress modes; Particle swarm optimization; Tensegrity structure.

1 Key Laboratory of Concrete and Prestressed Concrete Structures of Ministry of Education, and National Prestress Engineering Research Center, Southeast University, Nanjing 211189, China. Email: chenyao@seu.edu.cn
2 School of Civil Engineering, Southeast University, Nanjing 211189, China
3 Creative Design Engineering Lab, School of Engineering, University of Liverpool, London Campus, EC2A 1AG, UK. Email: pooya.sareh@livepool.ac.uk
4 Key Laboratory of Concrete and Prestressed Concrete Structures of Ministry of Education, and National Prestress Engineering Research Center, Southeast University, Nanjing 211189, China (corresponding author). Email: fengjian@seu.edu.cn

Introduction

Prestressed cable-strut structures have attracted considerable attention because of their novel configurations, excellent performance, lightweight, and high efficiency. These structures have become a hot spot in the field of space structures, showing great vitality and broad application prospects (Fest et al. 2004; Rhode-Barbarigos et al. 2010; Tibert and Pellegrino 2002). Compared with traditional truss and frame structures, prestressed cable-strut structures largely rely on initial prestresses to obtain or improve their overall stiffness (Chen and Feng 2012; Guest 2006; Sultan 2013). However, the strong coupling between their configurations and internal forces makes the design analysis more complicated (Chen et al. 2012; Zhang et al. 2009; Zhang et al. 2014). Therefore, morphology analysis of this type of structures is essential for the utilization and popularization of novel prestressed cable-strut structures in engineering design practice.

Prestressed cable-strut structures are generally composed of axially loaded members such as tension cables and compression struts (Chen et al. 2018; Li et al. 2016; Wang 1998). In fact, they are extended from the concept of tensegrity (Motro 2003; Wang 1998), and refer to a variety of structural forms, including tensegrity structures, cable dome structures, and cable truss structures (Guo and Zhou 2016; Quagliaroli et al. 2015; Zhang and Feng 2017). A common characteristic of these structures is that self-balancing prestresses exist in their members. However, according to the definition of tensegrity, tensegrity structures should be free-standing and self-balanced by certain connections of continuous cables and discontinuous struts (Chen et al. 2015; Wang 1998). Meanwhile, other cable-strut structures need to rely on external constraints or actions to be stable (e.g., cable dome structures), whereas the struts can be either discontinuous or continuous (Chen et al. 2019; Guo and Zhou 2016; Yuan and Dong 2003). Admittedly, the determination of relationships amongst initial configurations and feasible prestress

distributions is a key problem in the design of prestressed cable-strut structures. In general, after the initial configuration is determined, the morphology analysis of a cable-strut structure includes finding a feasible initial prestress distribution. This is also known as force-finding or form-finding. Over the past few decades, several analytical and computational methods have been developed to design and optimize the initial configurations of tensegrities, such as the dynamic relaxation method, the force density method, and finite element method (Estrada et al. 2006; Micheletti and Williams 2007; Motro 2003; Pagitz and Mirats Tur 2009; Zhang and Ohsaki 2006). Sultan et al. (2001) have pointed out that the general prestressability conditions of tensegrity structures can be analytically computed. Koohestani (2017) presented an analytical form-finding method for tensegrity structures, which could be useful and efficient for structures with high symmetry or regular configurations. Feng and Guo (2015) proposed a numerical method to determine the sole configuration of tensegrities with specified nodes. Li et al. (2010) adopted graph theory and presented a method to construct tensegrity structures from elementary cells. Yuan and Dong (2003) introduced the concept of integral self-stress states for finding the feasible prestress modes of large-scale prestressed cable-strut structures, which is based on double singular value decompositions on certain matrices. Lee et al. (2016) utilized the force density method and an automatic group selection for the members, followed by presenting an advanced form-finding process for truncated polyhedral tensegrities by using force density method combined with a genetic algorithm.

However, the involved form-finding process might be computationally expensive for complex structural geometry, particularly in the design of large-scale or long-span cable-strut structures with many nodes and members. Normally, these prestressed cable-strut structures have multiple self-stress states (Tran and Lee 2011), i.e., they have a number of independent self-stress states. Then, the initial prestresses of the members can be evaluated from the linear

combination of these self-stress states. However, it is generally difficult to compute a feasible prestress mode from many independent self-stress states, whereas some intractable questions need to be further concerned according to specified functions or performance of an actual project (Ali et al. 2010; Feng 2018). A simple example is that the obtained initial prestresses in the members should not only guarantee structural stability, but also satisfy specific conditions during design (e.g., symmetry, uniformity, and unilateral property). Consequently, the determination of feasible prestress distribution becomes a key point in developing prestressed cable-strut structures.

In fact, only a few studies have been performed on evaluating the optimal initial prestress distribution to stabilize a structure with a specified configuration, considering the unilateral property of members; that is, each cable should be in tension and each strut should be in compression (Quirant et al. 2003; Yuan and Dong 2003). After converting the original force-finding problems into optimization problems, some researchers have successfully introduced optimization algorithms to seek optimal prestress modes. Chen et al. (Chen et al. 2012a; Chen et al. 2012b) developed discrete optimization models for the form-finding and prestress stability analysis of predefined cable-strut structures, and adopted the ant colony system to search for feasible solutions. Xu and Luo (2010) performed the force-finding process of a tensegrity with cubic symmetry using the simulated annealing algorithm. Based on the simulated annealing combined with a stingy method, Zhang and Ohsaki (2011) evaluated the force distribution for prestressed pin-jointed structures and obtained the optimal locations for force measurements to achieve the highest accuracy of force identification. By using the force density method combined with a genetic algorithm, Lee et al. (Lee and Lee 2014; Tran et al. 2012; Tran and Lee 2011) introduced an advanced form-finding procedure for tensegrity structures and cable domes. Through an optimization process using the genetic algorithm, Koohestani and Guest (Koohestani 2015; Koohestani and Guest 2013) presented a novel approach for the determination of feasible

prestress modes and grouping of elements for tensegrities with specific geometries and multiple self-stress states. It is important to point out that, the involved force-finding process can be simplified by appropriate optimization models, whereas multiple sets of optimal solutions can be found (Xu et al. 2018). Nevertheless, in general, when the solution space is large, the corresponding optimization analysis becomes complicated and ineffective (Chen et al. 2012a). Recent studies have shown that the analytic relationships of force densities and integral self-stress states of symmetric prestressed cable-strut structures can be qualitatively obtained using symmetry (Chen et al. 2015; Chen et al. 2018; Zhang et al. 2009).

Here, the particle swarm optimization (PSO) algorithm is introduced to establish the optimal feasible prestress modes of prestressed cable-strut structures. A significance of this work is that qualitative analysis and optimization analysis are neatly combined, to effectively reduce the solution space and improve the force-finding of cable-strut structures. The fitness function is established by using the weight coefficient method, and the multi-objective optimization problem associated with the force-finding process is neatly converted into a single-objective optimization problem. Feasible prestress modes are optimized from the independent self-stress states and the integral self-stress states of the structure. The results of the PSO algorithm are compared with the respective results obtained from the conventional genetic algorithm and the simulated annealing algorithm. It is demonstrated that the proposed optimization model is a suitable and efficient procedure for the determination of feasible prestress modes of cable-strut structures with multiple self-stress states.

Initial Prestress Distribution of a Cable-Strut Structure Considering Integrity and Unilateral Conditions

First, the concepts and relations of independent self-stress states, integral self-stress states, and feasible prestress modes should be described, as these three prestress modes are pivotal to the force-finding analysis of cable-strut structures.

Independent self-stress states

Every self-stress state of a structure is a nominal vector of the internal forces of the members, which satisfies the self-equilibrium condition of the structure. In fact, there is one state or multiple independent states of self-stress for a prestressed cable-strut structure (Chen et al. 2015; Estrada et al. 2006; Tran and Lee 2010). These self-stress states only satisfy the nodal equilibrium (Yuan et al. 2007), without guaranteeing structural stability. In addition, either the unilateral conditions of the forces in the cables and struts, or the symmetry properties of the structure have not been considered.

For a given cable-strut structure with b members and N free nodes, the equilibrium equation of the structure can be written as

$$\boldsymbol{H}\boldsymbol{t} = \boldsymbol{P} \tag{1}$$

where $\boldsymbol{H}$ is the $3N \times b$ equilibrium matrix, $\boldsymbol{t}$ is the $b \times 1$ internal force vector, $\boldsymbol{P}$ is the $3N \times 1$ external load vector of free nodes, and certain degrees of freedom of the constrained nodes are excluded. Supposing that the rank of the matrix $\boldsymbol{H}$ is r, the structure has $s = b - r$ self-stress states. According to the equilibrium matrix theory (Pellegrino and Calladine 1986), the independent self-stress states $\boldsymbol{S}_1, \boldsymbol{S}_2, \ldots, , \boldsymbol{S}_S$ of the structure can be extracted from the null space of the equilibrium matrix $\boldsymbol{H}$ by the singular value decomposition (SVD) method or the Gauss

elimination method (Pellegrino 1993). Then, the initial prestress mode $\boldsymbol{t}_0$ of the structure can be evaluated from a reasonable combination of these independent self-stress states, expressed by

$$\boldsymbol{t}_0 = \boldsymbol{S}_1\alpha_1 + \boldsymbol{S}_2\alpha_2 + ... + \boldsymbol{S}_s\alpha_s = \boldsymbol{S}\boldsymbol{\alpha} \tag{2}$$

where the matrix $\boldsymbol{S} = [\boldsymbol{S}_1 \quad \boldsymbol{S}_2 \quad \cdots \quad \boldsymbol{S}_s]^{\mathrm{T}}$ represents the independent self-stress states of the structure, which contains *s* nominal basis vectors for the internal forces of the members. The nonzero vector $\boldsymbol{\alpha} = [\alpha_1 \quad \alpha_2 \quad \cdots \quad \alpha_s]^{\mathrm{T}}$ describes the corresponding combination coefficients of the self-stress states.

Integral self-stress states with full symmetry

For a cable-strut structure retaining a specific symmetry, the members being located in equivalent positions (i.e., on the same symmetry orbit) should be classified into the same group. In that case, the members of the same group necessarily have identical initial prestresses, which can be taken as the integrity condition of the members. Notably, the integral self-stress states consider the inherent symmetry of the structure and thus preserve the full symmetry. Moreover, they satisfy the equilibrium condition and the integrity condition. However, these self-stress states with full symmetry ignore the unilateral condition of the members (Chen et al. 2015; Yuan and Dong 2003).

Double singular value decomposition (DSVD) method is a conventional technique for solving the integral self-stress states of a structure (Yuan et al. 2007). The first application of SVD on the equilibrium matrix $\boldsymbol{H}$ is to obtain the self-stress states $\boldsymbol{S}$. The second application of SVD on the augmented matrix $[\boldsymbol{S} \quad -\boldsymbol{e}]$ is to compute the integral self-stress states, where the force matrix $\boldsymbol{e}$ reveals the distribution of normalized forces of the members from different groups.

In fact, recent studies have shown that the stiffness matrices and the equilibrium matrix can be transformed into block-diagonalized forms using group theory (Chen et al. 2015; Chen and Feng 2012; Koohestani and Kaveh 2010;

Raj and Guest 2006). For instance, on the basis of a group-theoretic approach, the equilibrium matrix $\boldsymbol{H}$ in the Cartesian coordinate system can be converted to a symmetry-adapted equilibrium matrix $\overline{\boldsymbol{H}}$

$$\overline{\boldsymbol{H}} = \boldsymbol{V}_P^{\mathrm{T}} \boldsymbol{H} \boldsymbol{V}_t = \mathrm{diag}\left[\overline{\boldsymbol{H}}^{(1\text{-}1)}, \cdots, \overline{\boldsymbol{H}}^{(1\text{-}l_1)}, \cdots, \overline{\boldsymbol{H}}^{(i\text{-}h)}, \cdots, \overline{\boldsymbol{H}}^{(\mu\text{-}1)}, \cdots, \overline{\boldsymbol{H}}^{(\mu\text{-}l_\mu)} \right] \tag{3}$$

where the matrices $\boldsymbol{V}_P$ and $\boldsymbol{V}_t$ represent the symmetry subspaces for the external loads $\boldsymbol{P}$ and the internal forces $\boldsymbol{t}$, respectively. In Eq. (3), diag( ) represents the diagonal form of a matrix, the positive integral $i \in [1, \mu]$, $h \in [1, l_i]$, and l_i and l_μ are the dimensions of the irreducible representations of Γ^i and Γ^μ. μ is the number of irreducible representations of a symmetry group. $\overline{\boldsymbol{H}}^{(i\text{-}h)}$ represents the h-th block of the symmetry-adapted equilibrium matrix associated with the i-th irreducible representation.

It can be noticed from Eq. (3) that the symmetry-adapted equilibrium matrix contains a few small-sized block matrices along the diagonal. Meanwhile, the symmetry properties of these block matrices along the diagonal decrease in sequence (Zingoni 2009). The first irreducible representation of a symmetry group always holds the full symmetry of the structure (Chen et al. 2015). Therefore, the integral self-stress states of the structure must be included in the first block matrix of the equilibrium matrix $\overline{\boldsymbol{H}}^{(1\text{-}1)}$. Because these block matrices are linearly independent, $\overline{\boldsymbol{H}}^{(1\text{-}1)}$ can be directly computed from the full symmetry subspaces, expressed as

$$\overline{\boldsymbol{H}}^{(1\text{-}1)} = (\boldsymbol{V}_P^{(1\text{-}1)})^{\mathrm{T}} \boldsymbol{H} \boldsymbol{V}_t^{(1\text{-}1)} \tag{4}$$

where $\boldsymbol{V}_P^{(1\text{-}1)}$ and $\boldsymbol{V}_t^{(1\text{-}1)}$, respectively included in the matrices of $\boldsymbol{V}_P$ and $\boldsymbol{V}_t$, are the full symmetry subspaces associated with the first irreducible representation $\Gamma^{1\text{-}1}$. Moreover, $\boldsymbol{V}_P^{(1\text{-}1)}$ is the orthogonal basis vector of the permutation matrix corresponding to the external load of nodes $\boldsymbol{R}_P$, which is given by

$$\boldsymbol{R}_P = \sum_{g \in G} \boldsymbol{R}_{P,g} \tag{5}$$

where g denotes an independent symmetry operation for the symmetric structure and G is the set of all independent symmetry operations. Each matrix $\boldsymbol{R}_{P,g}$ represents the permutation matrix of the external load vector $\boldsymbol{P}$ under the symmetry operation g (Chen and Feng 2012). Similarly, $\boldsymbol{V}_t^{(1-1)}$ is the orthogonal basis vector of the permutation matrix corresponding to the internal force vector of the members $\boldsymbol{R}_t$, which can be expressed as

$$\boldsymbol{R}_t = \sum_{g \in G} \boldsymbol{R}_{t,g} \tag{6}$$

where $\boldsymbol{R}_{t,g}$ represents the permutation matrix of the internal force vector $\boldsymbol{t}$ under the symmetry operation g. Then, the null space $\overline{\boldsymbol{S}}^{(1-1)}$ of the first block $\overline{\boldsymbol{H}}^{(1-1)}$ can be obtained using SVD, and satisfies

$$\overline{\boldsymbol{H}}^{(1-1)} \overline{\boldsymbol{S}}^{(1-1)} = \boldsymbol{0} \tag{7}$$

By combining Eq. (4) with Eq. (7), we have

$$\overline{\boldsymbol{H}}^{(1-1)} \overline{\boldsymbol{S}}^{(1-1)} = (\boldsymbol{V}_P^{(1-1)})^{\mathrm{T}} \boldsymbol{H} \boldsymbol{V}_t^{(1-1)} \overline{\boldsymbol{S}}^{(1-1)} = \boldsymbol{0} \tag{8}$$

Then, the integral self-stress states of the structure can be expressed as

$$\boldsymbol{S}' = \boldsymbol{V}_t^{(1-1)} \overline{\boldsymbol{S}}^{(1-1)} \tag{9}$$

Thus, Eq. (7) can be rewritten as

$$\overline{\boldsymbol{H}}^{(1-1)} \overline{\boldsymbol{S}}^{(1-1)} = (\boldsymbol{V}_P^{(1-1)})^{\mathrm{T}} \boldsymbol{H} \boldsymbol{S}' = \boldsymbol{0} \tag{10}$$

Eqs. (7, 10) indicate that it must be satisfied for $\overline{\boldsymbol{H}}^{(1-1)} \overline{\boldsymbol{S}}^{(1-1)} = \boldsymbol{0}$ on condition that $\boldsymbol{H}\boldsymbol{S}' = \boldsymbol{0}$. As a consequence, Eq. (7) is a necessary condition for the nodal equilibrium of the structure. In other words, the existence of the null space $\overline{\boldsymbol{S}}^{(1-1)}$ of the first block $\overline{\boldsymbol{H}}^{(1-1)}$ of the symmetry-adapted equilibrium matrix (i.e., $\overline{\boldsymbol{H}}^{(1-1)} \overline{\boldsymbol{S}}^{(1-1)} = \boldsymbol{0}$) is a necessary condition for the self-equilibrium of a symmetric cable-strut structure (i.e., $\boldsymbol{H}\boldsymbol{S}' = \boldsymbol{0}$). As expected, the integral self-stress states of the cable-strut structure can be directly obtained from the first block matrix of the equilibrium matrix (Chen et al. 2015).

Feasible prestress modes

The definition of feasible prestress modes is stricter than those of the self-stress states and the integral self-stress states. A feasible prestress mode simultaneously satisfies the equilibrium condition, the integrity condition, and unilateral condition of the members (Yuan and Dong 2003).

For a structure with a single integral self-stress state, it is necessary to verify whether the self-stress state meets the unilateral condition of the members; that is, each cable should be in tension and each strut should be in compression (Chen et al. 2019; Yuan and Dong 2003). If this unilateral condition is satisfied (i.e., the force of a cable *i* should be $\boldsymbol{t}_i > 0$, and that of a strut *j* should be $\boldsymbol{t}_j < 0$), the single integral self-stress state is exactly the feasible prestress mode of the structure. Otherwise, there is no feasible prestress mode, and thus the structural configuration should be redefined. On the other hand, for a structure with multiple independent integral self-stress states, each integral self-stress state generally does not satisfy the unilateral condition (Chen et al. 2015). Therefore, the feasible prestress mode should be obtained by a linear combination of the integral self-stress states, expressed as

$$\boldsymbol{t_0} = \boldsymbol{S}_1^{'}\alpha_1^{'} + \boldsymbol{S}_2^{'}\alpha_2^{'} + ... + \boldsymbol{S}_{s'}^{'}\alpha_{s'}^{'} = \boldsymbol{S}^{'}\boldsymbol{\alpha}^{'} \tag{11}$$

where s' is the number of integral self-stress states, and the nonzero vector $\boldsymbol{\alpha}^{'} = [\alpha_1^{'} \quad \alpha_2^{'} \quad \cdots \quad \alpha_{s'}^{'}]^{\mathrm{T}}$ denotes the corresponding combination coefficients of the integral self-stress states. Figure 1 describes the relations among the feasible prestress mode, the independent self-stress states, and the integral self-stress states. We can notice that the feasible prestress mode of a cable-structure can be obtained from either the independent self-stress states using Eq. (2), or the integral self-stress states using Eq. (11).

Calculation of Integral Feasible Prestress Modes for Cable-Strut Structures

The particle swarm optimization (PSO) algorithm

The particle swarm optimization algorithm is one of the most popular evolutionary algorithms proposed by Eberhart and Kennedy (Eberhart and Kennedy 2002). It simulates the flight foraging behavior of birds, and achieves optimal goals through collective cooperation. Because of its high efficiency and robustness, the particle swarm optimization algorithm has been an important tool for solving practical problems, and has been widely utilized in science and engineering (Fu et al. 2012; Lee and Kim 2013; Robinson and Rahmatsamii 2004; Wang et al. 2016).

The basic idea of PSO is that a particle flies at a certain velocity in the searching space, and its velocity is dynamically adjusted according to its own flight experience and the flight experience of its companion. A fitness function is established to evaluate whether the particle is *good* or *bad*. The optimization algorithm exploits a random solution to initialize a group of random particles, then the optimal solution is found by iteration. In each iteration step, the particle is updated by tracking two extremes: the individual extremum (i.e., *pbest*) and the global extremum (*gbest*). *Pbest* is the best solution found in the particle itself, and *gbest* is the optimal solution of all particles in the whole particle swarm during the searching process. Each particle constantly changes its velocity in the solution space, so that it can fly to the area directed at *pbest* and *gbest* as far as possible.

Mathematical model based on integral self-stress states

For a given configuration with certain symmetry, the initial prestress mode of the structure can be derived from integral self-stress states using Eq. (11). The solution of the combination coefficient $\boldsymbol{\alpha}$ can be converted to a multivariable optimization problem. To make full use of the structural materials, the internal forces $\boldsymbol{t}_0$ of the members should be uniformly distributed. Therefore, to evaluate the prestress uniformity, a function $u(\boldsymbol{\alpha})$ with

respect to $\boldsymbol{\alpha}$ is defined as the variance of the initial prestress mode

$$u(\boldsymbol{\alpha}) = \frac{\mathrm{var}(\mathrm{abs}(\boldsymbol{t}_0))}{\mathrm{var}(\mathrm{abs}(\boldsymbol{t}_0)) + 1} \tag{12}$$

where the function is denoted as a normalized value with a specific range, $0 \le u(\boldsymbol{\alpha}) < 1$, $\mathrm{abs}(\boldsymbol{t}_0)$ represents the absolute value of each entry in the column vector $\boldsymbol{t}_0$, and $\mathrm{var}(\ )$ denotes variance. In fact, as a cable-strut structure is symmetric and consists of a total number of *n* types of members, a generalized form of the variance of initial prestresses can be expressed as

$$\mathrm{var}(\mathrm{abs}(\boldsymbol{t}_0)) = \sqrt{\frac{1}{n}\sum_{i=1}^{n}\left(\left|\boldsymbol{t}_{0,i}(\boldsymbol{\alpha})\right| - \frac{1}{n}\sum_{j=1}^{n}\left|\boldsymbol{t}_{0,j}(\boldsymbol{\alpha})\right|\right)^2} \tag{13}$$

where $\boldsymbol{t}_{0,i}(\boldsymbol{\alpha})$ and $\boldsymbol{t}_{0,j}(\boldsymbol{\alpha})$ respectively denote the prestress modes of the *i*-th and *j*-th types of members determined by the coefficient vector $\boldsymbol{\alpha}$. On the basis of the integral self-stress states, the unilateral condition of the members should be met; it requires that all the cables are in tension and all the struts are in compression. Then, the optimization problem corresponding to finding the integral feasible prestress mode is

$$\begin{aligned} &\min \ u(\boldsymbol{\alpha}) \\ &\text{s.t.} \ \ t_i > 0 \quad i \in \text{cable} \\ &\qquad t_j < 0 \quad j \in \text{bar} \\ &\qquad \alpha_i \in [-1, 1] \end{aligned} \tag{14}$$

However, when a cable-strut structure has a relatively large number of members, the above optimization problem tends to be either unsolvable or difficult to converge. This is because the objective function and the constraint conditions in Eq. (14) cannot be satisfied simultaneously. Thereafter, Eq. (14) is modified to consider the constraint conditions into the objective function. Here, we denote a parameter M as the number of members that do not satisfy the unilateral condition, and

$$g(\boldsymbol{\alpha}) = M/b \tag{15}$$

where the function $0 \le g(\boldsymbol{\alpha}) < 1$ is utilized to compute the proportion of those *M* specific members among all the *b* members. Therefore, the unilateral condition is converted into the minimum optimization problem of $g(\alpha)$. By obtaining the combination coefficient $\boldsymbol{\alpha}$ that minimizes both $u(\boldsymbol{\alpha})$ and $g(\boldsymbol{\alpha})$, the integral feasible prestress mode can be solved. It turns out that the evaluation of the integral feasible prestress mode is transformed into a multi-objective optimization problem.

In addition, to perform a much fairer comparison and ensure the convergence of the above-mentioned optimization problem, the combination coefficients of the integral prestress modes should be normalized

$$\|\boldsymbol{\alpha}\|_2 = 1 \tag{16}$$

where $\| \ \|_2$ represents the 2-norm of a vector.

In the standard PSO algorithm, all particles have a fitness function to evaluate the current position. For the constrained optimization problem, the penalty function method is used to construct the fitness function. Based on this idea, the weight coefficient method is utilized to construct the fitness function, and the modified fitness function is written as

$$F(\boldsymbol{\alpha}) = \omega_1 u(\boldsymbol{\alpha}) + \omega_2 g(\boldsymbol{\alpha}) \tag{17}$$

where ω_1 and $\omega_2 \in (0, 1)$ are the corresponding weight coefficients. It should be noted that these two objective functions are not completely equivalent. The integral feasible prestress modes must strictly satisfy the unilateral condition, while the condition of internal force uniformity needs not to be strictly satisfied. Thus, ω_2 should be larger than ω_1.

Consequently, the optimization model based on the integral self-stress states can be expressed as

$$\begin{aligned} &\min \ \ \omega_1 u(\boldsymbol{\alpha}) + \omega_2 g(\boldsymbol{\alpha}) \\ &\text{s.t.} \ \ \alpha_i \in [-1,1], \text{and} \ \ \|\boldsymbol{\alpha}\|_2 = 1 \end{aligned} \tag{18}$$

Mathematical model based on independent self-stress states

Admittedly, when a structure is asymmetric (without integral self-stress states) or it has a very small number of independent self-stress states, the integral feasible prestress mode can be directly obtained from independent self-stress states using Eq. (2). In order to guarantee the same prestress for the members of the same type, all the members need to be manually classified. Note that the members have been divided into n groups ($n \le b$), and the $b \times n$ matrix $\boldsymbol{u}$ can be written as

$$\boldsymbol{u} = [\boldsymbol{u}_1 \ \ \cdots \ \ \boldsymbol{u}_i \ \ \cdots \ \ \boldsymbol{u}_n] \tag{19}$$

where the $b \times 1$ basis vector $\boldsymbol{u}_i$ ($i \in [1, n]$) represents the distribution of the i-th group of members, defined as

$$\boldsymbol{u}_i = [0 \ \ 1 \ \ \cdots \ \ 1 \ \ 0 \ \ 1 \ \ \cdots \ \ 0 \ \ 0]^{\mathrm{T}} \tag{20}$$

In the vector $\boldsymbol{u}_i$, each entry corresponding to the i-th group of members is taken as 1, and those of the other groups of members are 0. Therefore, the initial prestress of each group of members can be separated by

$$\boldsymbol{t}_0^i = (\boldsymbol{t}_0) \circ \boldsymbol{e}_i \tag{21}$$

where $\boldsymbol{t}_0^i$ is the initial prestress force of the i-th group of members and the symbol $\circ$ represents the multiplication of entries in the corresponding positions of the two vectors. According to the symmetry properties of the structure, members in the same group have identical prestresses. In this model, the variance is used as an evaluation index of the uniformity of the initial prestresses, expressed as

$$f(\boldsymbol{\alpha}) = \sum_{i=1}^{n} \mathrm{var}(\boldsymbol{t}_0^{\,i}) \tag{22}$$

where $\mathrm{var}(\ )$ represents variance, $f(\boldsymbol{\alpha})$ is the sum of variances of the prestress force for all groups of members.

In addition, this function is slightly modified to lie in a specific range [0, 1), given by

$$f'(\boldsymbol{\alpha}) = \frac{f(\boldsymbol{\alpha})}{f(\boldsymbol{\alpha})+1} \tag{23}$$

Therefore, considering the unilateral condition of the members, the corresponding optimization problem of finding the integral feasible prestress process can be stated as follows

$$\begin{aligned} &\min\ f'(\boldsymbol{\alpha}) \\ &\text{s.t.}\quad t_i > 0 \quad i \in \text{cable} \\ &\qquad t_j < 0 \quad j \in \text{bar} \\ &\qquad \alpha_i \in [-1,1], \text{and } \|\boldsymbol{\alpha}\|_2 = 1 \end{aligned} \tag{24}$$

Similarly, the penalty function method is transformed and considered in the optimization model, where the modified fitness function is expressed as

$$H(\boldsymbol{\alpha}) = \omega_1' f'(\boldsymbol{\alpha}) + \omega_2' g(\boldsymbol{\alpha}) \tag{25}$$

where ω_1' and $\omega_2' \in (0,1)$ are the corresponding weight coefficients. The self-stress states are the standard orthogonal basis of the null space of the equilibrium matrix, so the value of $f(\boldsymbol{\alpha})$ is generally small. Therefore, to ensure the minimum value of the evaluation function, the weight coefficients should satisfy $1 > \omega_1' > \omega_2' > 0$. Notably, each weight coefficient can be basically determined through the value of the involved function at the first steps, to guarantee that the function value at the first iteration steps is neither large nor very close to 0.

Therefore, the integral feasible prestress mode optimization model based on the self-stress states can be expressed as

$$\begin{aligned} &\min\ \omega_1' f'(\boldsymbol{\alpha}) + \omega_2' g(\boldsymbol{\alpha}) \\ &\text{s.t.}\quad \alpha_i \in [-1,1], \text{and } \|\boldsymbol{\alpha}\|_2 = 1 \end{aligned} \tag{26}$$

To further describe the above-mentioned optimization model using either the integral self-stress states (Eq. (18)) or the self-stress states (Eq. (26)), a flowchart for the proposed PSO approach is given in Fig. 2. Importantly, as shown in Fig. 2(a), the stability of cable-strut structures with specific geometry should be evaluated after feasible prestress modes are obtained through the optimization process. In fact, it can be effectively evaluated by the positive

definiteness of the tangent stiffness matrix $\boldsymbol{K}_T$ of the structure with optimized prestresses (Chen and Feng 2012; Guest 2006), which is given by

$$\boldsymbol{K}_T = \boldsymbol{K}_E + \boldsymbol{K}_G \tag{27}$$

where $\boldsymbol{K}_E$ is the linear stiffness matrix, and $\boldsymbol{K}_G$ is the geometric stiffness matrix contributed by the optimized feasible prestresses $\boldsymbol{t}$.

Illustrative Examples

In this section, illustrative examples are presented to identify the feasible prestress modes using the above optimization models. In the proposed PSO-based approach, different parameters can be utilized to improve the computational efficiency of the algorithm. In order to facilitate comparison, the number of particles is uniformly 400 and the maximum number of iterations is chosen to be 800. In the model based on the integral self-stress states, the weight coefficients are taken as $\omega_1 = 0.1$, and $\omega_2 = 0.5$. In the model based on the self-stress states, the weight coefficients are taken as $\omega_1^{'} = 0.5$, and $\omega_2^{'} = 0.2$.

To verify the feasibility and accuracy of the proposed method, numerical analysis using conventional optimization methods is also carried out and the obtained results are compared with the corresponding PSO-based results. All these numerical examples are implemented in MATLAB on a laptop with 1.8 GHz i7-8550U CPU and 16 GB RAM.

Two-dimensional cable-strut structures

A simple 2D hexagonal cable-strut structure is first studied, where the structural configuration is shown in Fig. 3(a). The structure consists of six nodes and fifteen members. It holds D_3 symmetry and remains invariant under three 3-fold rotations and three 2-fold rotations. According to the symmetry property, the structure has $n = 3$ groups of members, whereas the symbol C1 represents the outer circumferential cables, C2 represents the additional internal

cables, and B1 represents the struts.

Numerical analysis shows that this structure has $s = 6$ self-stress states and $s' = 2$ integral self-stress states. Using the mathematical model based on the integral self-stress states $\boldsymbol{S}'$, the feasible prestress mode $\boldsymbol{t}_0$ is obtained from the particle swarm optimization process, listed in Table 1.

Table 1 shows that the initial prestresses of the C1 cables are positive, while those of the B1 struts are negative. However, the internal cables of group C2 have no prestress. The optimization result shows that, with the feasible prestress mode listed in Table 1, the structure shown in Fig. 3(a) is equivalent to the conventional hexagonal cable-strut structure shown in Fig. 3(b). It demonstrates that the proposed optimization method for calculating the feasible prestress mode is effective.

Levy cable dome with C_{8v} symmetry

Figure 4 shows a typical Levy cable dome structure with C_{8v} symmetry and a total of $n = 7$ groups of members. The structure is composed of 26 pin-joints and 65 members, and eight outmost nodes are constrained in all three directions. It can be observed that, because of the inherent C_{8v} symmetry, this cable dome structure would remain invariant under eight 8-fold rotations and eight mirror operations. As shown in Fig. 4(b), the members JS1 and JS2 denote the ridge cables, XS1 and XS2 denote the diagonal cables, HS denotes the hoop cables, and VP1 and VP2 denote the vertical struts.

This cable dome has a diameter of 48m (Xi et al. 2011), whereas the hoop cables (denoted by HS) with a diameter of 32m are arranged inside. The lengths of the vertical struts are $l_{\mathrm{VP1}} = 9.238\mathrm{m}$ and $l_{\mathrm{VP2}} = 8.574\mathrm{m}$, respectively. First-order analysis shows that the rank of the 54×65 equilibrium matrix $\boldsymbol{H}$ is calculated to be 54, and thus the

structure has $s = 11$ independent self-stress states and $s^{'} = 1$ integral self-stress states.

Because this structure has no internal mechanisms and possesses only a single integral self-stress state, the PSO model based on the integral self-stress states can directly find the feasible prestress to make the dome structure stable. No additional iterative computation is needed. However, to further describe the advantages of considering symmetry and integral self-stress states, here we deliberately perform a force-finding analysis using $s = 11$ independent self-stress states (rather than the integral self-stress state). After 114 iterations of the PSO algorithm, the value of the fitness function $H(\boldsymbol{\alpha}) = 0.0011$ (see Eq. (25)), and the combination coefficient of the self-stress states derived from the optimal solution *gbest* is

$$\begin{aligned}\boldsymbol{\alpha}_{gbest} = [\ & 0.036601 \quad 0.083320 \quad -0.082354 \quad -0.045776 \quad -0.060229 \quad -0.052405 \\ & 0.014467 \quad 0.093164 \quad -0.059894 \quad 0.043112 \quad 0.034399\ ]^{T}\end{aligned} \tag{28}$$

According to the optimal combination coefficient worked out by the PSO algorithm, a feasible prestress mode of the Levy cable dome can be obtained, which satisfies the symmetry condition and unilateral condition of the members. Note that the optimal result is in complete agreement with the integral self-stress state and the numerical results obtained by Xi et al (2011), as shown in Fig. 5.

On the other hand, to evaluate the robustness of the presented PSO-based force-finding method, Fig. 6(a-b) shows the variations of the fitness function value using the PSO algorithm with different number of particles and different weigh coefficient. Moreover, Fig. 6(c-d) respectively show the results obtained by the well-known genetic algorithm (El-Lishani et al. 2005; Zhang and Feng 2017), and the simulated annealing algorithm (Xu and Luo 2010), where the optimization model given by Eq. (26) keeps identical.

It can be noticed from Fig. 6(a) that the convergence process of the PSO algorithm is relatively stable, as the fitness function value is very close to the optimal solution after 62 iterations. The number of the particles has a slight effect on the results. For this optimization mode with 11 independent variables, 200 particles are sufficient to accurately obtain the optimal solution. Note that a very small number of particles lead to getting a local optimal solution or premature convergence, as illustrated by the dash lines in Fig. 6(a). Besides, Fig. 6(b) shows that the optimal solution and the convergence performance of the PSO algorithm are not sensitive to the value of ω_2, which mainly affects the obtained results at the first iteration steps. This is because the optimal value of $g(\boldsymbol{\alpha})$ keeps zero (see Eq. (15)).

Fig. 6(c-d) shows that the same optimal solution can be achieved by the genetic algorithm and the simulated annealing algorithm. Notably, the simulated annealing algorithm takes much more iteration steps, although it is easy to implement. The convergence of the genetic algorithm is similar to the PSO method, where the optimal solution can be obtained in less than 150 steps. However, each iteration step of the generic algorithm costs a long time because of the reproduction procedure and the crossover and mutation procedure (Zhang and Feng 2017). Actually, complete force-finding process based on the PSO method, the genetic algorithm, and the simulated annealing algorithm takes 17.618s, 48.965s, and 318.087s, respectively. Further, a series of main parameters of the genetic algorithm need to be gradually specified through a trial-and-error process to guarantee stable convergence and acceptable computational consumption (Zhang and Feng 2017). As a result, compared with the conventional genetic algorithm and the simulated annealing algorithm, the PSO approach is not only feasible but also effective for the force-finding of cable-strut structures.

Kiewitt cable dome with C_{8v} symmetry

Figure 7 displays a 3D Kiewitt cable dome with 81 members and 36 pin-joints, where a total of 18 boundary nodes are constrained along *X*, *Y*, and *Z* directions. This structure also retains C_{8v} symmetry, and it remains invariant under eight 8-fold rotations and eight mirror operations. All the members can be classified into *n*=9 groups using symmetry properties. The span of the structure is 48m, and the diameter of the hoop cables HS is 32m. The height of the lower vertical struts VP1 and the upper vertical struts VP2 are 9.238m and 8.574m, respectively. As shown in Fig. 7(b), the members JS1, JS2, and JS3 denote the ridge cables, and XS1, XS2, and XS3 denote the corresponding diagonal cables. The rank of the 54×81 equilibrium matrix is $r=54$. Therefore, through first-order analysis and symmetry analysis, the structure has $s=27$ self-stress states, and $s^{'}=3$ integral self-stress states.

It is worth mentioning that, when using the optimization model based on the self-stress states, the optimization process cannot find a feasible solution. This is because such a cable dome has a large number of independent self-stress states. As the number of self-stress states increases, the solution space for the optimization process increases significantly, which makes the algorithm difficult to converge. Hence, for this type of cable-strut structures with numerous self-stress states, the optimization model based on the integral prestress mode should be adopted.

Based on the integral self-stress states, the calculated results of the Kiewitt cable dome are shown in Table 2. It can be observed that the feasible prestress mode of the structure can be effectively obtained from $s^{'}=3$ integral self-stress states. The obtained prestress mode satisfies both the symmetry condition and the unilateral condition of the members.

Conclusions

Based on the particle swarm optimization algorithm, two optimization models for solving feasible prestress modes of prestressed cable-strut structures with multiple self-stress states are proposed. Both optimization models utilize the weight coefficient method to convert multi-objective optimization into a single-objective optimization problem. For a cable-strut structure with either asymmetry or a small number of self-stress states, the optimization model based on self-stress states can be directly utilized for calculation. Importantly, for a symmetric cable-strut structure with multiple self-stress states, using the optimization model based on the integral self-stress states can significantly reduce the computational complexity and ensure the convergence of the iteration process.

Acknowledgements

This work has been supported by the National Natural Science Foundation of China (Grant No. 51978150 and No. 51850410513), Southeast University "Zhongying Young Scholars" Project, and the Fundamental Research Funds for the Central Universities. The first author would like to acknowledge financial support from the Alexander von Humboldt-Foundation for his academic research at Max-Planck-Institut für Eisenforschung GmbH, Germany. The authors are grateful to the anonymous reviewers for their valuable comments.

References

Ali, N., Rhode-Barbarigos, L., Albi, A., and Smith, I. (2010). "Design optimization and dynamic analysis of a tensegrity-based footbridge." *Engineering Structures*, 32(11), 3650-3659.

Chen, Y., and Feng, J. (2012). "Generalized eigenvalue analysis of symmetric prestressed structures using group theory." *Journal of Computing in Civil Engineering*, 26(4), 488-497.

Chen, Y., Feng, J., Lv, H., and Sun, Q. (2018). "Symmetry representations and elastic redundancy for members of tensegrity structures." *Composite Structures*, 203, 672-680.

Chen, Y., Feng, J., Ma, R., and Zhang, Y. (2015). "Efficient symmetry method for calculating integral prestress modes of statically indeterminate cable-strut structures." *Journal of Structural Engineering, ASCE*, 141(10), 04014240.

Chen, Y., Feng, J., and Wu, Y. (2012a). "Prestress stability of pin-jointed assemblies using ant colony systems." *Mechanics Research Communications*, 41, 30-36.

Chen, Y., Feng, J., and Wu, Y. (2012b). "Novel form-finding of tensegrity structures using ant colony systems." *Journal of Mechanisms and Robotics-Transactions of the ASME*, 4(3), 031001.

Chen, Y., Sun, Q., and Feng, J. (2018). "Group-theoretical form-finding of cable-strut structures based on irreducible representations for rigid-body translations." *International Journal of Mechanical Sciences*, 144, 205-215.

Chen, Y., Yan, J., Sareh, P., and Feng, J. (2019). "Nodal flexibility and kinematic indeterminacy analyses of symmetric tensegrity structures using orbits of nodes." *International Journal of Mechanical Sciences*, 155, 41-49.

Eberhart, R., and Kennedy, J. "A new optimizer using particle swarm theory." *International Symposium on MICRO*

Machine and Human Science, 39-43.

El-Lishani, S., Nooshin, H., N., Disney, and P., D. (2005). "Investigating the statical stability of pin-jointed structures using genetic algorithm." *International Journal of Space Structures*, 20(1), 53-68.

Estrada, G. G., Bungartz, H. J., and Mohrdieck, C. (2006). "Numerical form-finding of tensegrity structures." *International Journal of Solids and Structures*, 43(22-23), 6855-6868.

Feng, X. (2018). "An investigation on optimal initial self-stress design of tensegrity grid structures." *International Journal of Steel Structures*, 1-16.

Feng, X., and Guo, S. (2015). "A novel method of determining the sole configuration of tensegrity structures." *Mechanics Research Communications*, 69, 66-78.

Fest, E., Shea, K., and Smith, I. (2004). "Active tensegrity structure." *Journal of Structural Engineering*, 130(10), 1454-1465.

Fu, Y., Ding, M., and Zhou, C. (2012). "Phase angle-encoded and quantum-behaved particle swarm optimization applied to three-dimensional route planning for UAV." *IEEE Transactions on Systems, Man, and Cybernetics - Part A: Systems and Humans*, 42(2), 511-526.

Guest, S. D. (2006). "The stiffness of prestressed frameworks: A unifying approach." *International Journal of Solids and Structures*, 43(3-4), 842-854.

Guo, J., and Zhou, D. (2016). "Pretension simulation and experiment of a negative Gaussian curvature cable dome." *Engineering Structures*, 127, 737-747.

Koohestani, K. (2015). "Automated element grouping and self-stress identification of tensegrities." *Engineering Computations*, 32(6), 1643-1660.

Koohestani, K. (2017). "On the analytical form-finding of tensegrities." *Composite Structures*, 166, 114-119.

Koohestani, K., and Guest, S. D. (2013). "A new approach to the analytical and numerical form-finding of tensegrity structures." *International Journal of Solids and Structures*, 50(19), 2995-3007.

Koohestani, K., and Kaveh, A. (2010). "Efficient buckling and free vibration analysis of cyclically repeated space truss structures." *Finite Elements in Analysis and Design*, 46(10), 943-948.

Lee, K. B., and Kim, J. H. (2013). "Multiobjective particle swarm optimization with preference-based sort and its application to path following footstep optimization for humanoid robots." *IEEE Transactions on Evolutionary Computation*, 17(6), 755-766.

Lee, S., Gan, B. S., and Lee, J. (2016). "A fully automatic group selection for form-finding process of truncated tetrahedral tensegrity structures via a double-loop genetic algorithm." *Composites Part B Engineering*, 106, 308-315.

Lee, S., and Lee, J. (2014). "Form-finding of tensegrity structures with arbitrary strut and cable members." *International Journal of Mechanical Sciences*, 85, 55-62.

Li, H., Zhang, H., Zheng, Y., and Zhang, L. (2016). "A peridynamic model for the nonlinear static analysis of truss and tensegrity structures." *Computational Mechanics*, 57(5), 843-858.

Li, Y., Feng, X., Cao, Y., and Gao, H. (2010). "Constructing tensegrity structures from one-bar elementary cells." *Proceedings of the Royal Society A-Mathematical Physical and Engineering Sciences*, 466(2113), 45-61.

Micheletti, A., and Williams, W. O. (2007). "A marching procedure for form-finding for tensegrity structures." *Journal of mechanics of materials and structures*, 2(5), 857-882.

Motro, R. (2003). *Tensegrity: Structural Systems for the Future*, Kogan Page Science, Elsevier, London and Sterling, VA.

Pagitz, M., and Mirats Tur, J. M. (2009). "Finite element based form-finding algorithm for tensegrity structures."

International Journal of Solids and Structures, 46(17), 3235-3240.

Pellegrino, S. (1993). "Structural computations with the singular value decomposition of the equilibrium matrix." *International Journal of Solids and Structures*, 30 (21), 3025-3035.

Pellegrino, S., and Calladine, C. R. (1986). "Matrix analysis of statically and kinematically indeterminate frameworks." *International Journal of Solids and Structures*, 22(4), 409-428.

Quagliaroli, M., Malerba, P. G., Albertin, A., and Pollini, N. (2015). "The role of prestress and its optimization in cable domes design." *Computers & Structures*, 161, 17-30.

Quirant, J., Kazi-Aoual, M. N., and Motro, R. (2003). "Designing tensegrity systems: the case of a double layer grid." *Engineering Structures*, 25(9), 1121-1130.

Raj, R. P., and Guest, S. D (2006). "Using Symmetry for Tensegrity Form-Finding." *Journal of the International Association for Shell and Spatial Structures*, 47, 245-252.

Rhode-Barbarigos, L., Hadj Ali, N. B., Motro, R., and Smith, I. F. C. (2010). "Designing tensegrity modules for pedestrian bridges." *Engineering Structures*, 32(4), 1158-1167.

Robinson, J., and Rahmatsamii, Y. (2004). "Particle swarm optimization in electromagnetics." *IEEE Trans Antennas Propag*, 52(2), 397-407.

Sultan, C. (2013). "Stiffness formulations and necessary and sufficient conditions for exponential stability of prestressable structures." *International Journal of Solids and Structures*, 50(14-15), 2180-2195.

Sultan, C., Corless, M., and Skelton, R. E. (2001). "The prestressability problem of tensegrity structures: some analytical solutions." *International Journal of Solids and Structures*, 38(30-31), 5223-5252.

Tibert, A. G., and Pellegrino, S. (2002). "Deployable tensegrity reflectors for small satellites." *Journal of Spacecraft and Rockets*, 39(5), 701-709.

Tran, H. C., and Lee, J. (2010). "Self-stress design of tensegrity grid structures with exostresses." *International Journal of Solids and Structures*, 47(20), 2660-2671.

Tran, H. C., and Lee, J. (2011). "Form-finding of tensegrity structures with multiple states of self-stress." *Acta Mechanica*, 222(1-2), 131-147.

Tran, H. C., Park, H. S., and Lee, J. (2012). "A unique feasible mode of prestress design for cable domes." *Finite Elements in Analysis and Design*, 59, 44-54.

Wang, B. (1998). "Cable-strut systems: Part II - Cable-strut." *Journal of Constructional Steel Research*, 45(3), 291-299.

Wang, B., Wang, S., Zhou, X., and Watada, J. (2016). "Two-stage multi-objective unit commitment optimization under hybrid uncertainties." *IEEE Transactions on Power Systems*, 31(3), 2266-2277.

Xi, Y., Xi, Z., and Qin, W. H. (2011). "Form-finding of cable domes by simplified force density method." *Proceedings of the Institution of Civil Engineers - Structures and Buildings*, 164(3), 181-195.

Xu, X., and Luo, Y. Z. (2010). "Force finding of tensegrity systems using simulated annealing algorithm." *Journal of Structural Engineering*, 136(8), 1027-1031.

Xu, X., Wang, Y., and Luo, Y. (2018). "Finding member connectivities and nodal positions of tensegrity structures based on force density method and mixed integer nonlinear programming." *Engineering Structures*, 166, 240-250.

Yuan, X. F., Chen, L., and Dong, S. L. (2007). "Prestress design of cable domes with new forms." *International Journal of Solids and Structures*, 44(9), 2773-2782.

Yuan, X. F., and Dong, S. L. (2003). "Integral feasible prestress of cable domes." *Computers & Structures*, 81(21), 2111-2119.

Zhang, J. Y., Guest, S. D., and Ohsaki, M. (2009). "Symmetric prismatic tensegrity structures. Part I: Configuration and stability." *International Journal of Solids and Structures*, 46(1), 1-14.

Zhang, J. Y., and Ohsaki, M. (2006). "Adaptive force density method for form-finding problem of tensegrity structures." *International Journal of Solids and Structures*, 43(18-19), 5658-5673.

Zhang, J. Y., and Ohsaki, M. (2011). "Force identification of prestressed pin-jointed structures." *Computers & Structures*, 89(23), 2361-2368.

Zhang, L., Li, Y., Cao, Y., and Feng, X. (2014). "Stiffness matrix based form-finding method of tensegrity structures." *Engineering Structures*, 58, 36-48.

Zhang, P., and Feng, J. (2017). "Initial prestress design and optimization of tensegrity systems based on symmetry and stiffness." *International Journal of Solids and Structures*, 106, 68-90.

Zingoni, A. (2009). "Group-theoretic exploitations of symmetry in computational solid and structural mechanics." *International Journal for Numerical Methods in Engineering*, 79(3), 253-289.

Tables

Table 1 Feasible prestress mode of the 2D cable-strut structure

Member group	Prestress mode of t_0 using PSO	Integral self-stress states S'	
		S_1'	S_2'
C1	0.01751	– 0.06712	0.33691
C2	$<10^{-6}$	– 0.20052	– 0.16767
B1	– 0.01751	0.41443	– 0.04649
Relationship between t_0 and S'	$t_0 = 0.0372S_1' + 0.0445S_2'$		

Table 2 Computational results of the cable dome with Kiewitt type

Type	JS1	JS2	JS3	XS1	XS2	XS3	HS	VP1	VP2
S_1'	– 0.19780	0.02231	– 0.07685	0.01653	– 0.11690	– 0.07685	– 0.13856	– 0.08180	0.15912
S_2'	– 0.07920	0.13126	0.03445	0.18774	– 0.04200	0.03445	0.15593	– 0.06159	– 0.07133
S_3'	– 0.14347	0.11820	– 0.00132	– 0.16494	0.13214	– 0.00132	– 0.00887	– 0.01933	0.00273
t_0	0.12373	0.05163	0.08298	0.03541	0.10895	0.08298	0.18663	– 0.10164	– 0.17181
Relationship between t_0 and S'	$t_0 = 0.15653S_1' + 0.40544S_2' - 0.90072S_3'$								

Figures

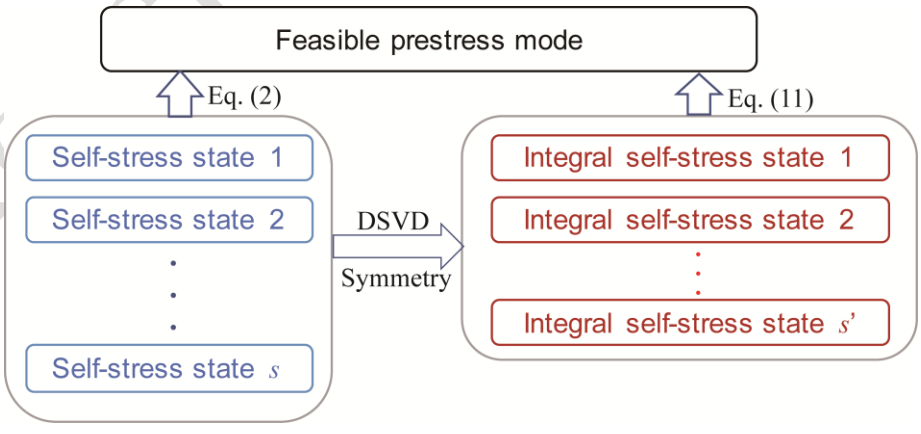

Fig. 1. Feasible prestress mode obtained from the independent self-stress states and the integral self-stress states

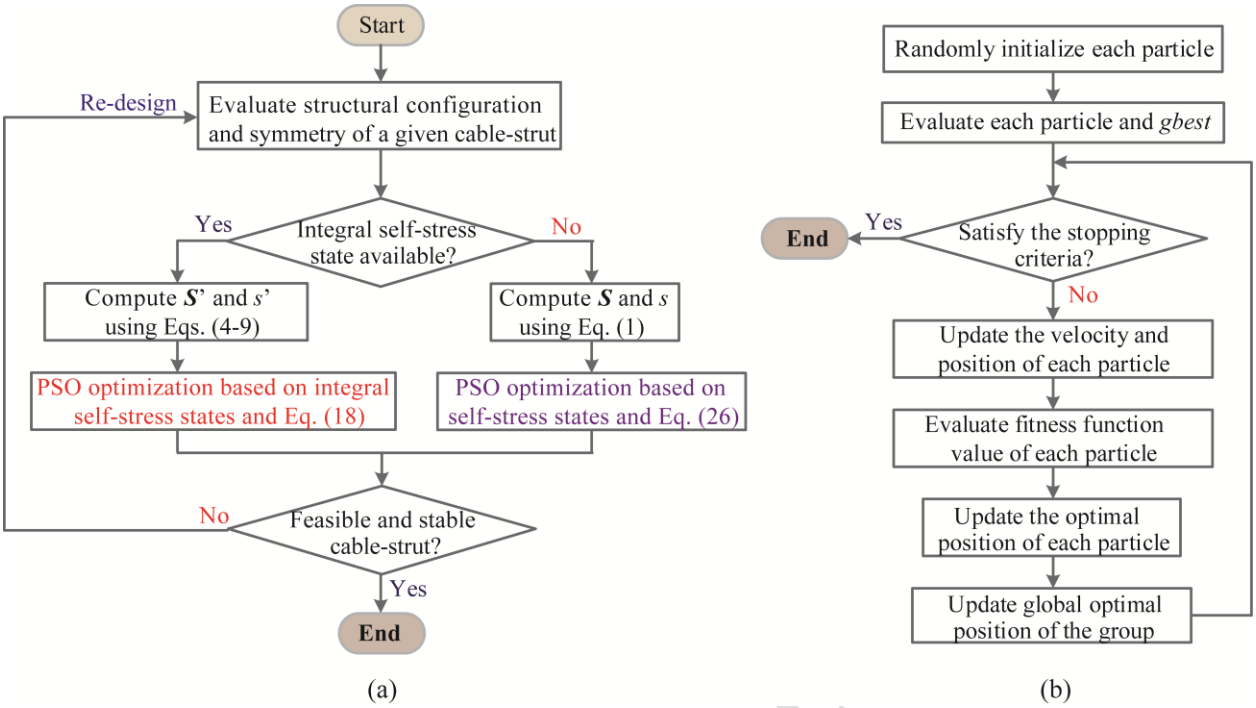

Fig. 2. Finding feasible prestress modes using PSO: (a) flowchart of force-finding process for the two optimization models; (b) flowchart of the PSO algorithm

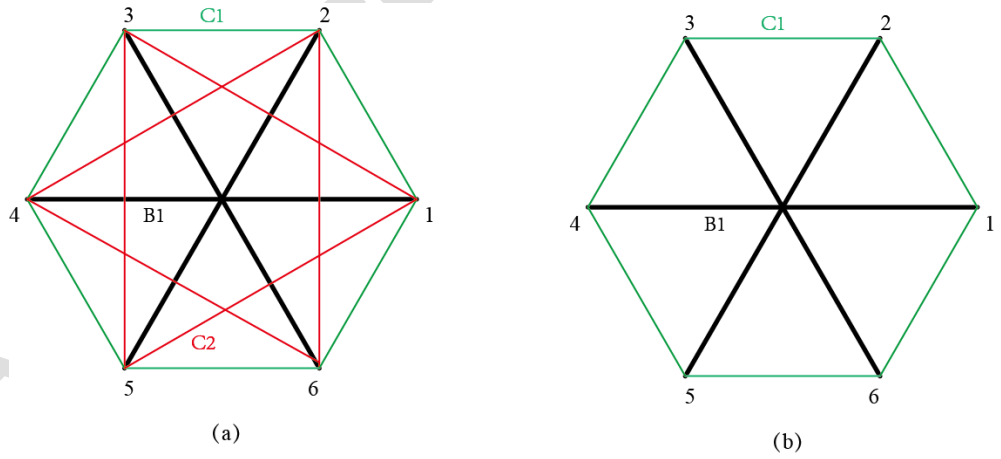

Fig. 3. Two-dimensional hexagonal cable-strut structures: (a) with additional internal cables; (b) without internal cables

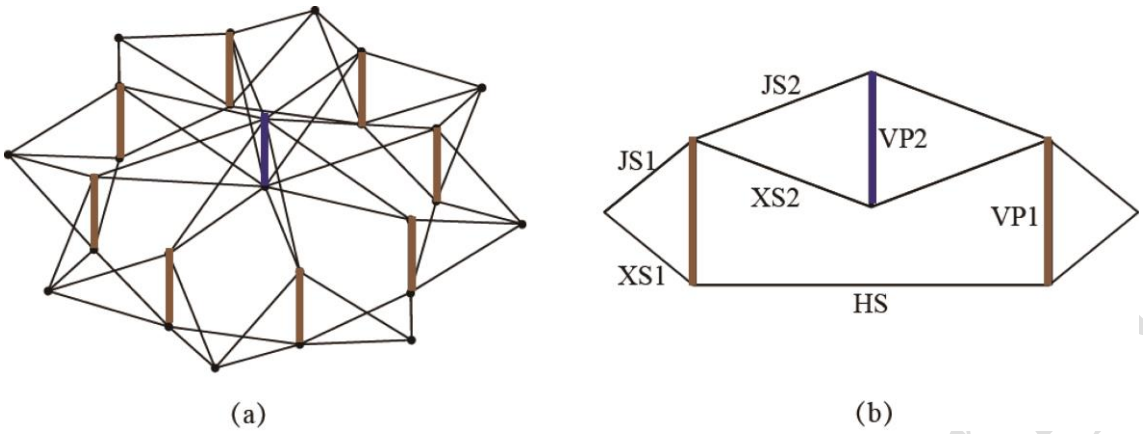

Fig. 4. Levy cable dome with C_{8v} symmetry: (a) 3D view; (b) different groups of members in section view

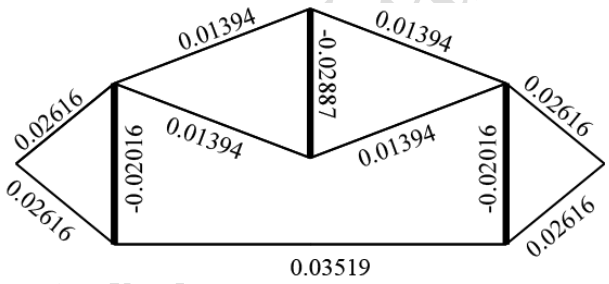

Fig. 5. Integral feasible prestress distribution of C_{8v} symmetric Levy cable dome

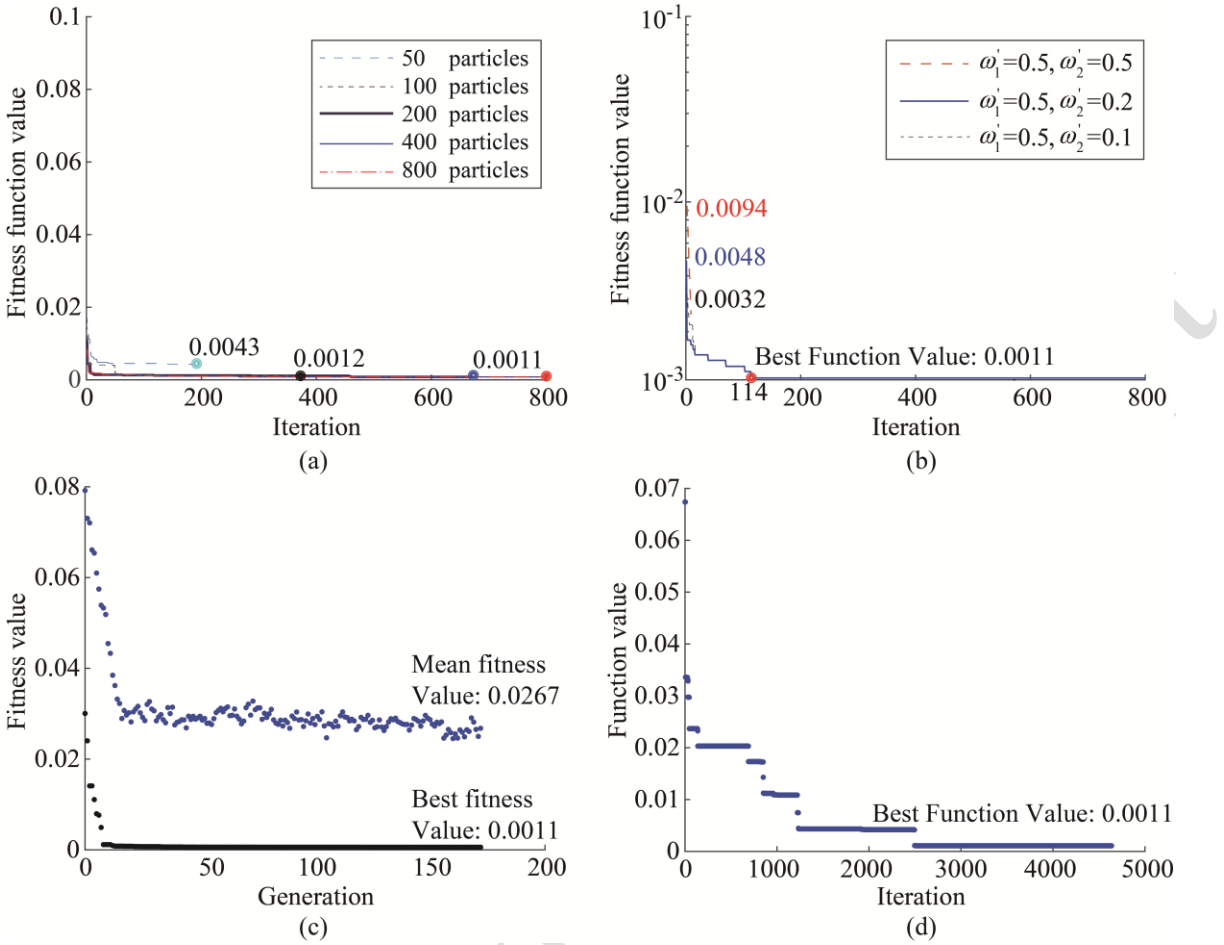

Fig. 6. Variations of the fitness function value along the iteration process: (a) PSO algorithm with different number of particles; (b) PSO algorithm with different weigh coefficient ω_2'; (c) genetic algorithm; (d) simulated annealing algorithm

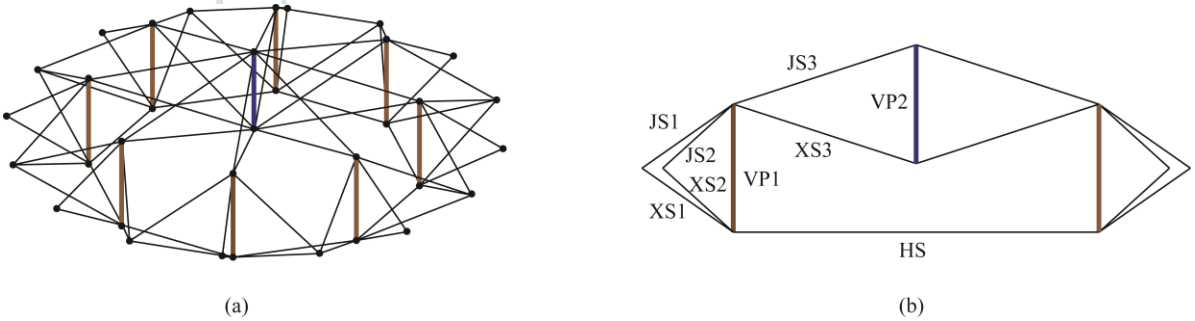

Fig. 7. A C_{8v} symmetric cable dome with Kiewitt type: (a) 3D view; (b) n = 9 groups of members illustrated in the section view